JOHNS HOPKINS UNIVERSITY Applied Physics Laboratory
Laurel MD 20723-6099

A1F(2)02-U-079
ICY0243X
November 20, 2002

To: S. L. Murchie

From: L. M. Howser

Subject: Responsivity Results for the CONTOUR Spectrograph

References: (1) L. M. Howser, "Preliminary Responsivity Results for the CONTOUR Spectrograph," A1F(2)02-U-048, July 2002.

(2) L. M. Howser, "Measurements of the Attenuator for the CRISP Test Equipment," A1F(2)02-U-082, October 2002.

(3) L. M. Howser, "Measurement of Brightness Samples with the CRISP Sensor," A1F(2)02-U-086, November 2002.

Summary

Preliminary spectrograph responsivity calculations were based on low-resolution calibration data for the CONTOUR test equipment. Recently, higher resolution data have been received. The responsivity of the CONTOUR spectrograph has been recalculated using this new calibration data. An overview of the calibration data is presented, along with the results of the calculations. The responsivity of the spectrograph is about one half of the predicted value across the spectrum.

Introduction

The CONTOUR Remote Imager and Spectrograph (CRISP) is one of the instruments on the CONTOUR spacecraft. The IR spectrograph contains a 256x256 HgCdTe array. The array is illuminated through a slit that provides a two-dimensional image. One dimension of the image is spatial, with a field-of-view of about 0.86°. The other image dimension is spectral, measuring the IR spectrum from 800 nm to 2500.

Accurate knowledge of the responsivity of the spectrograph is required for analysis of the flight data. The responsivity is defined as a measure of the system response (digital counts) per input radiance. To support this responsivity analysis, a series of integrating sphere images were collected during the calibration of the instrument. These data include a series of uniformly-flooded images at various light levels.

The various light levels were generated using the integrating sphere and apertures. A high-resolution calibration of this test equipment was completed this summer. This calibration measured the spectral radiance of the equipment under full power (no attenuation) and with various attenuator settings. These spectral radiance data and the sensor images have been combined to compute the responsivity of the CRISP instrument.

In addition to computing the responsivity, the sphere images have been used to estimate the scatter within the CRISP sensor. Reference (3) discusses the scatter within the brightness sample data. The same technique, using the signals in the dark rows, has been used to estimate the scatter in the sphere images.

Integrating Sphere Test Conditions

The test setup for the integrating sphere tests included a white integrating sphere with two inputs: a halogen lamp and a xenon lamp. Each lamp had a knife-edge attenuator between the lamp and the integrating sphere. Thus, each lamp was attenuated individually. During these tests, the attenuators were commanded from 255 (closed, background image) to 0 (open). When both lamps were used, the two attenuators were commanded to the same value. When only one lamp was used, the attenuator for the unused lamp was commanded to 255.

The data from the test sequence 355_CSBML_WFR_02 were used in these analyses. These files are from calibration tests performed after the instrument's environmental tests. Three series of data were collected for this test: with the halogen and xenon lamps individually and jointly. Examples of the images collected during this testing are shown in Figure 1. Images from the halogen, xenon, and joint test conditions are on the left of the plot. The aperture was set to 130 in all three cases. Average horizontal traces from each of the images are plotted on the right of the figure. This figure shows that the halogen lamp had more power than the xenon lamp and the xenon lamp caused sharp spikes in the images. These sharp spikes at 1325 nm in the halogen and joint traces are caused by the intersection of the two spectral filters of the CRISP sensor. The dark rows are shown in the top of each image. These rows appear to have signal only from the background. However, it will be shown that the signal in these rows increases linearly with scene (image) intensity.

Sphere Calibration Data

Responsivity is a measure of the system output (counts) per unit input (radiance in $W/cm^2/sr$). To compute the responsivity of a system we need to accurately know the input to the system. For the integrating sphere tests:

$$\text{input radiance} = r(L) * t_a(L) * t_w(L)$$

where $r(L)$ = radiance of source (from the lamp(s) through the integrating sphere)
$t_a(L)$ = transmission of the attenuator, and
$t_w(L)$ = transmission of the test equipment window.

The spectral radiance from the source was measured over the summer. These measurements were performed with no attenuation (setting 0) and at various attenuator settings. Thus, for this analysis the product of the lamp radiance and attenuator transmission was used from the calibration measurements.

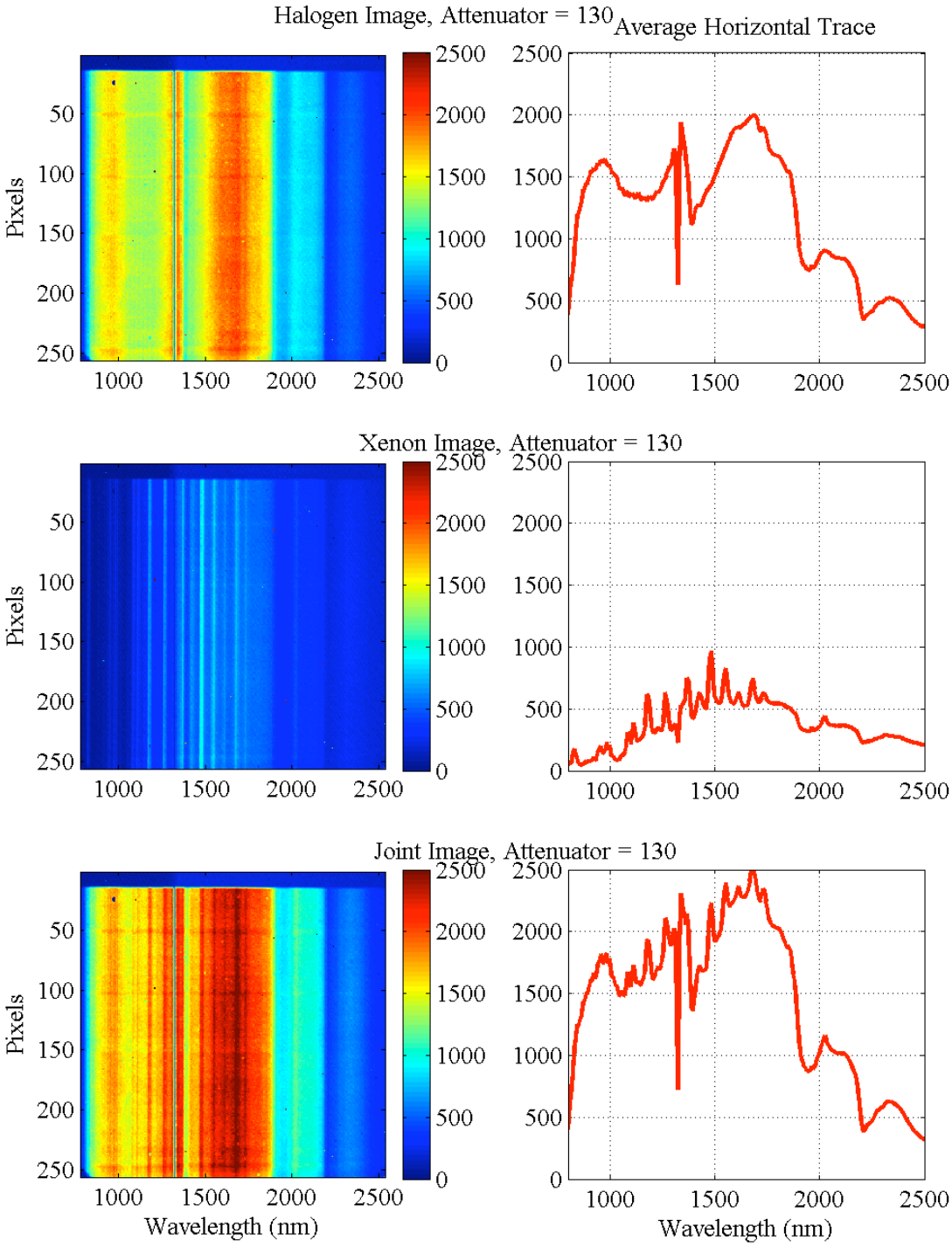

Figure 1 Example images from the integrating sphere tests. The three images on the left show examples from the halogen, xenon, and joint lamp tests. The traces on the right show the structure of the spectrograph response. The dark (unexposed) rows are shown in the top of each image.

The window transmission is shown in Figure 2. This curve was taken from the appendix of the master calibration record. The data were provided at a resolution of 5 nm. The transmission loss at about 1385 nm is also seen in the halogen and joint images of Figure 1. Because the spectral band of the CRISP instrument extends slightly beyond 2500 nm, the window transmission curve was extrapolated to provide transmission data spanning the band of interest.

Calibration data of the integrating sphere are shown in Figure 3. The halogen, xenon, and joint data are shown with no attenuation. Clearly, the halogen lamp dominates the signal in this spectral band. The xenon lamp added sharp spikes to the spectrum, also seen in the spectrograph images.

There are some concerns about the accuracy of the sphere calibration for use in the responsivity calculations. The CRISP sensor was tested in December of 2001. All of the images used in this analysis were collected at that time. Between the time of the CRISP tests and the sphere calibration, the halogen lamp burned out. This lamp was replaced by another lamp from the same manufacturer. Thus, the change in halogen lamps raises the question of the accuracy of the calibration. Similarly, between the CRISP tests and the sphere calibration, the xenon lamp showed signs of wear.

Reference (2) summarizes the data from the sphere calibration. Between the CRIPS measurements and the sphere calibration, the photometer in the sphere measured an overall signal change of greater than a factor of 2 in the halogen data for the OPEN attenuator position. This change is attributed to the different bulbs used during the CRISP measurements and the sphere calibration. A much smaller change in signal ($\approx$ 15%) was seen in the xenon data. To give accurate responsivity results, the sphere spectra were scaled by the ratio of the OPEN signals measured during the CRISP and sphere calibration tests. (The spectra in Figure 3 have been scaled by the signal ratios.)

In addition to the overall signal change, a change in the transmission of the attenuator was seen. Data in reference (2) show that the transmissions of the attenuators were not consistent between the CRISP tests and the sphere calibration. While most attenuator positions show less than a 10% change in transmission between the two tests, a factor of 2 change in transmission was seen at one attenuator position in the halogen data. This change in transmission could be attributed to either a different positioning of the bulb with respect to the attenuator, or uncertain knowledge of the attenuator position during CRISP testing. These differences in transmission were corrected by scaling the measured sphere spectra by the transmission ratios.

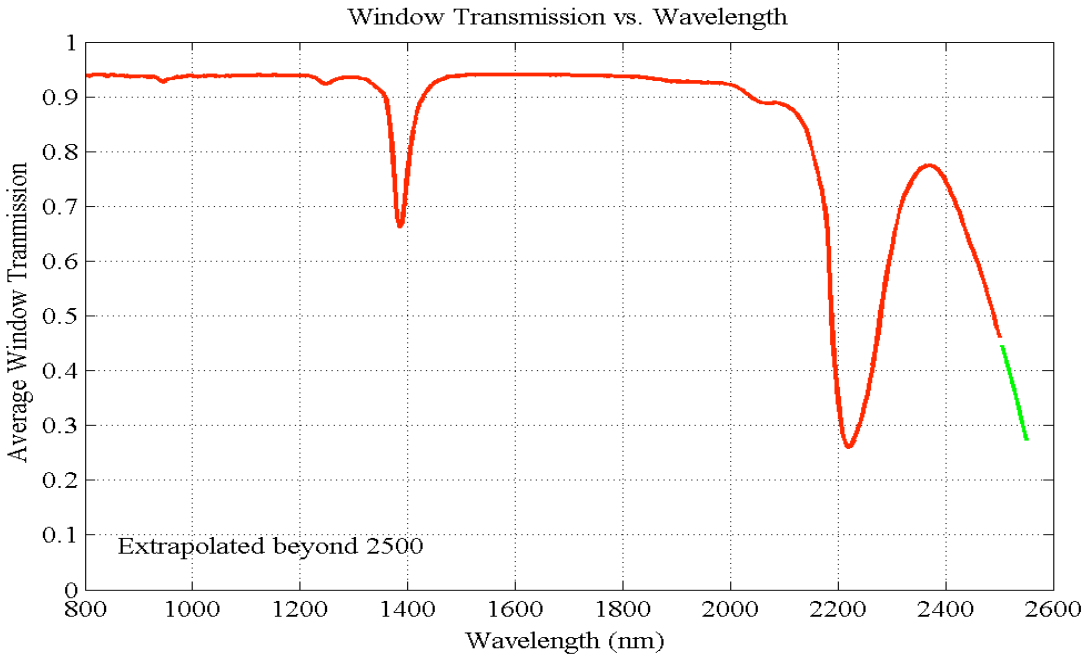

Figure 2 Test Chamber Window Transmission

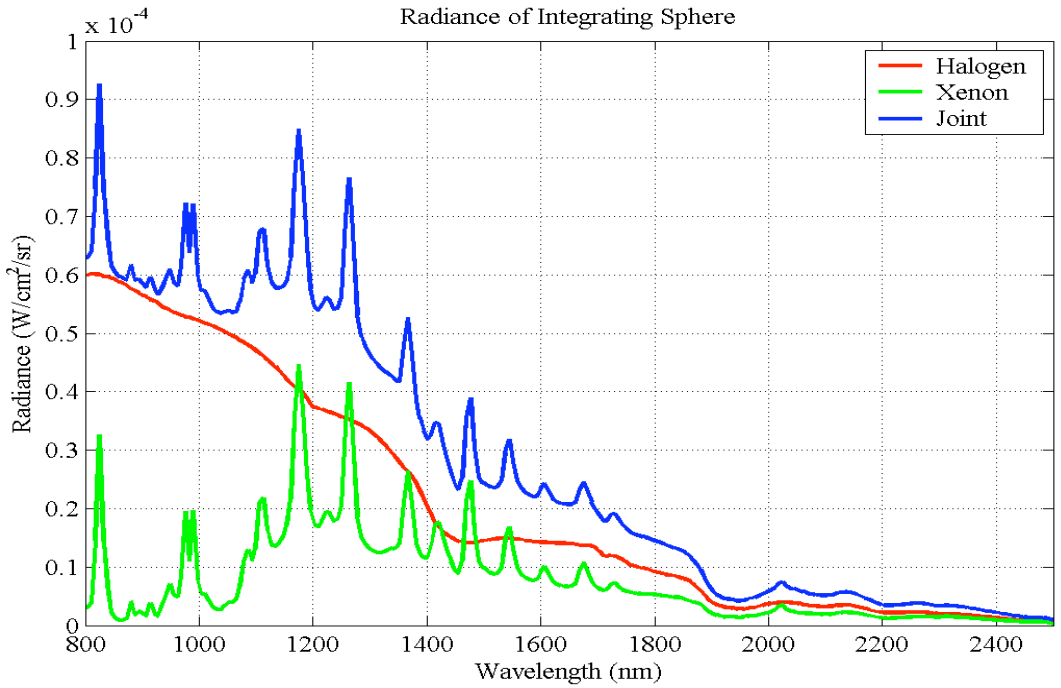

Figure 3: Measured radiance of integrating sphere. The radiance from the three lamp configurations is shown. The data in these plots were collected without attenuation. The halogen lamp is the major source of signal in this spectral band.

The effect of the attenuators can be seen in Figure 4. The measured radiance of the halogen lamp is shown for 12 attenuator positions, from fully open (0) to fully closed (255).

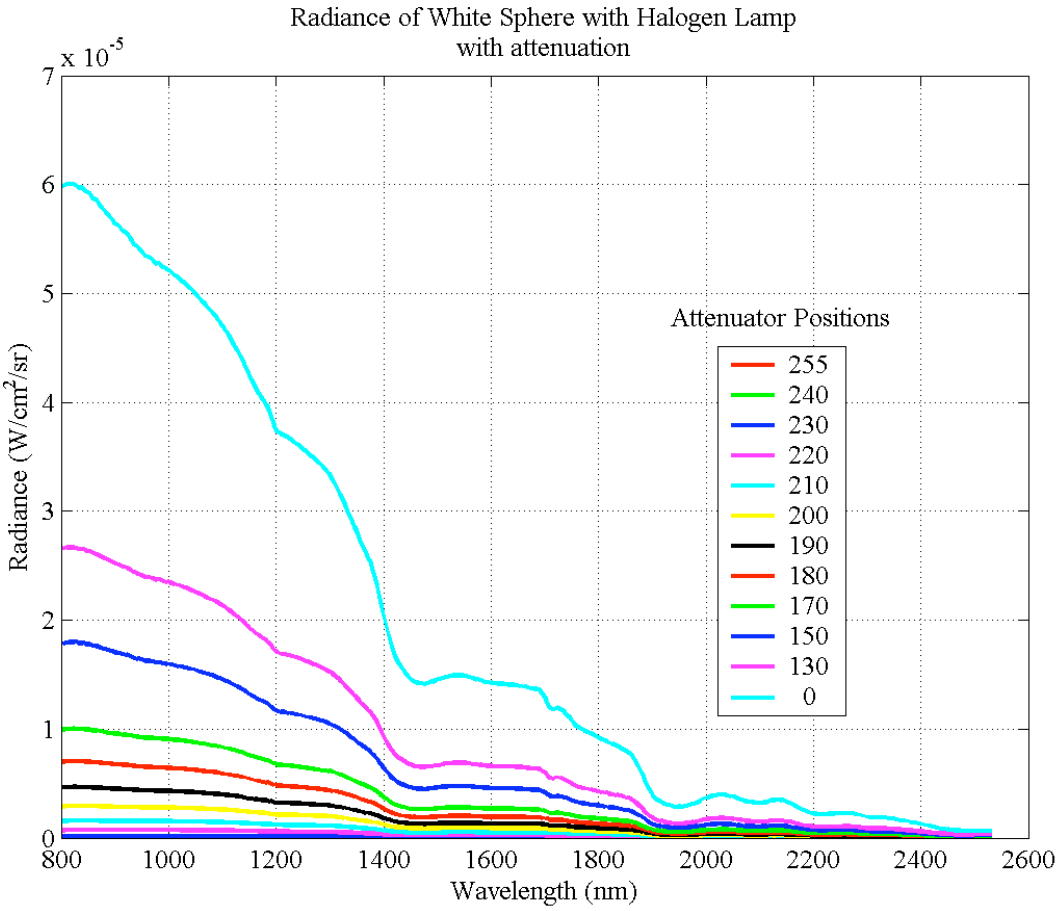

Figure 4 Radiance of halogen lamp with attenuation measured during the sphere calibration. The effect of the attenuator is seen in the reduction of the measured radiance.

Scatter Results

The dark (unexposed) rows of the image, shown in Figure 1, have some signal above the background. These rows are shown in Figure 5. The top of this figure shows an average trace from all attenuator positions for the 3 Hz images. The background image (CLOSED attenuator) has been subtracted from these traces. The flatness of the highest signal, from the 0 (OPEN) attenuator position, shows that the sensor saturated at that light level. The bottom plot in the figure shows the average from the dark rows of the same sensor images. This figure shows that as the scene intensity increases (top plot), the signal in the dark row also

increases (bottom plot). However, the spectra of the dark rows do not match the spectra from the scene. These observations indicate that the signals in the dark rows are caused by scatter within the sensor. A low-pass filter has been applied to the dark signal traces to reduce the effect of noise.

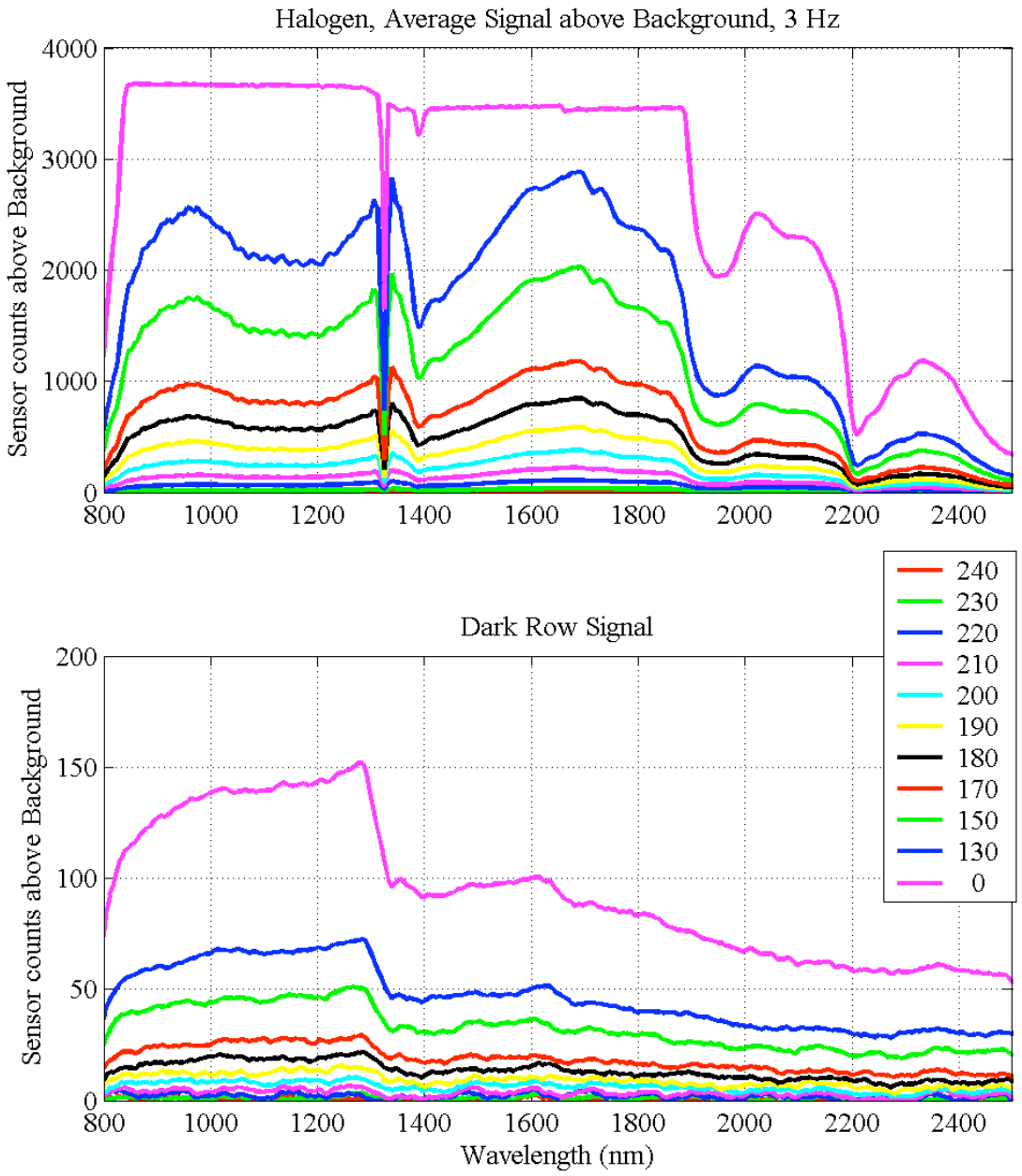

Figure 5: Average traces from the sphere images (top) and from the corresponding dark rows (bottom). These traces show that the signal in the dark rows increase as the scene intensity increases.

Figure 6 summarizes some of the data from Figure 5. In this plot, the average in the dark rows (bottom plot of Figure 5) is plotted against the average in the scene (top plot of Figure 5). The red circles are the data from the 11 attenuator positions; the line is a linear fit to the data. This plot shows that the average in the dark rows increases linearly with the average in the scene, up to the saturation limit. After saturation of the reported scene intensity, the signal in the dark rows continues to increase.

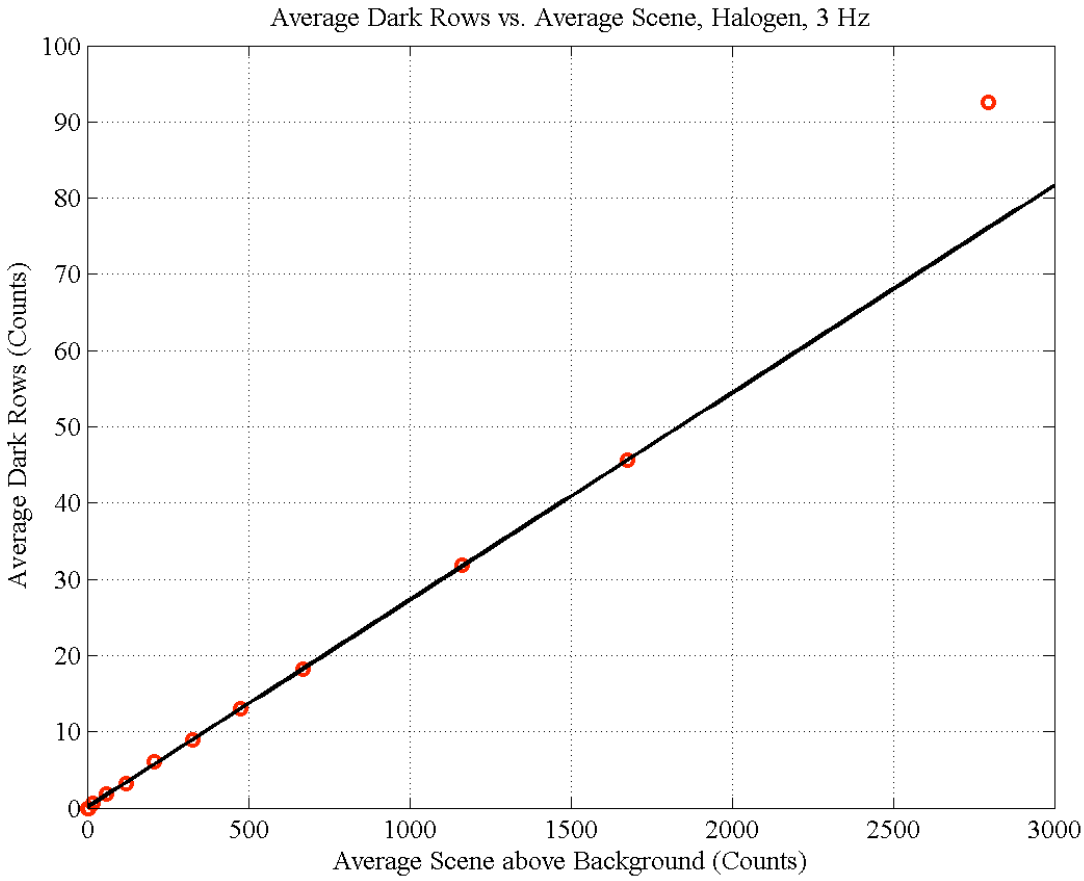

Figure 6: Average of dark rows versus average in scene. This plot shows the linear relationship between the signal in the dark rows and the scene intensity. The sensor was saturated when the highest point in the plot was collected.

Because the signal in the dark rows appears to provide a good measure of the scatter in the CRISP sensor, this signal can be used to remove the effect of scatter. To remove the effect of scatter, the average of the top 8 rows of the image was computed. A low-pass filter (7 pixels wide) was then applied to this average dark row to reduce noise. This low-passed, average dark row (estimate of scatter) was then subtracted from the sphere data. This subtraction is discussed in the next section.

Responsivity Results

The final responsivity equation is:

responsivity = (delta image counts) / (delta radiance),

or

$$\text{responsivity} = \frac{\text{sphere image} - \text{background} - \text{scatter}}{[\, r(L) * t_a(L)\,] * t_w(L) - \text{ambient radiance}}$$

The background image (attenuator = 255) and ambient radiance must be subtracted to give an accurate measurement of the responsivity. The estimated scatter, discussed in the previous section, is also subtracted in this equation.

Thus, the responsivity of the instrument is computed by subtracting the background and scatter data from the sphere image, and then dividing by the input radiance. Figure 7 shows the halogen lamp responsivity curves for six attenuator positions. The data from the six curves lie close together, indicating a consistent measurement of the lamp radiance with attenuation. The spikes around 2200 nm correspond to the region of lower transmission in the window. The predicted responsivity (from Jeff Warren) is plotted in black dots. The computed responsivity is about a factor of 1.7 below the predicted results.

Additional processing was required for the xenon data. Because the xenon lamp had sharp spikes in the spectrum, a misalignment of the measured calibration spectrum and the CRISP sensor waveband became visible. Initially, when the responsivity was computed (dividing the sensor spectrum by the sphere spectrum), the resulting curve had a series of large positive and negative spikes. These spikes were caused by a shift between the two wavelengths. To correct this effect, I modified the expected wavelength of the sensor. Previous calibration of the CRISP wavelength (by Jim Bell) produced the result that the wavelengths ranged from 769 nm to 2526 nm with a resolution of 6.89 nm / pixel. The wavelengths I used to match the calibration data were from 784 nm to 2532 nm with a resolution of 6.855 nm / pixel. (Since we only had two datasets, I could not determine which spectrum was accurate. I could only shift one spectrum with respect to the other to align the two.)

The CRISP FPA is slightly rotated with respect to the sensor grating. Along the length of a column, a rotation of about 1 pixel is visible. This rotation does not affect the halogen data because of the smooth spectrum. However, the rotation of the array causes the sharp spikes in the xenon data to spread into more than one wavelength. This spreading has a slight effect on the computed responsivity.

The measured sphere radiance spectrum also had a finer resolution than the CRISP spectrum. I applied a slight low-pass filter (equivalent to 1 CRISP pixel width) to smooth the radiance spectrum. The responsivity curve computed using this method is shown in Figure 8. These results are very similar to the halogen results, again about a factor of 2 below the predicted results.

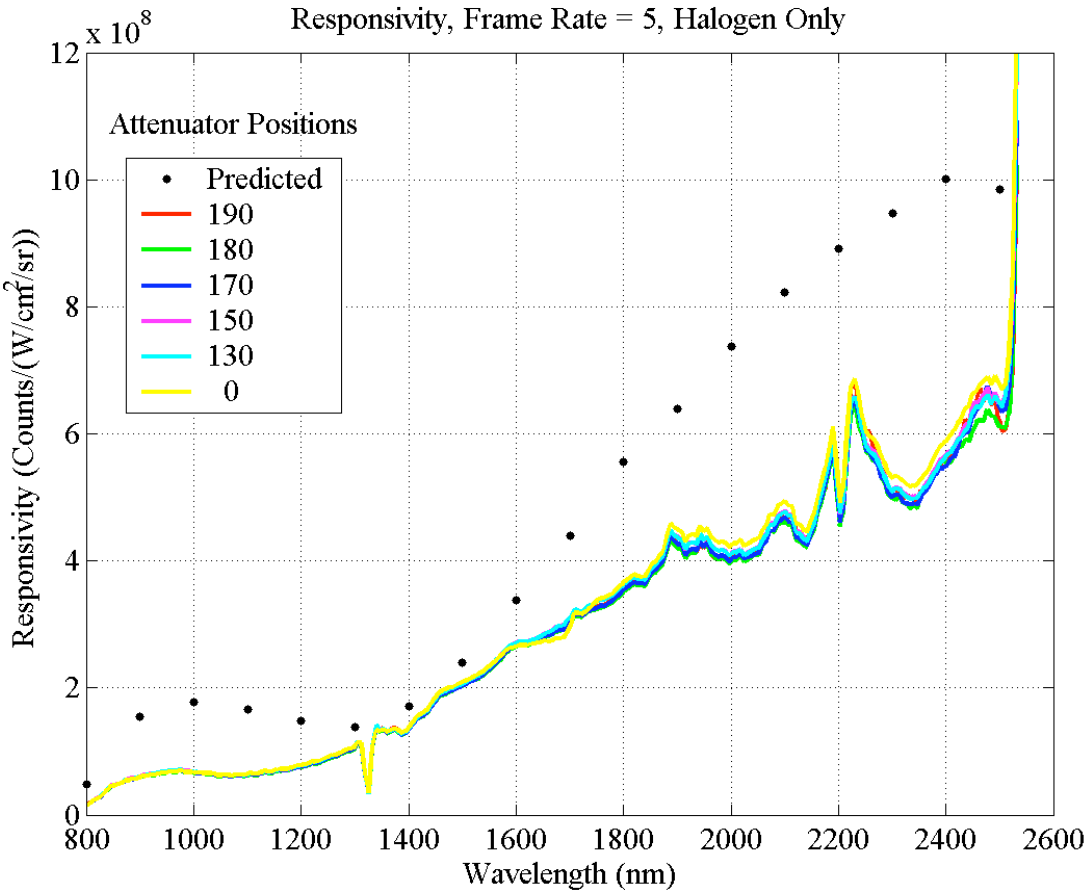

Figure 7: Responsivity of CRISP using halogen lamp. Data from the 6 attenuator settings show consistent results. The measured responsivity is about 60% of the predicted.

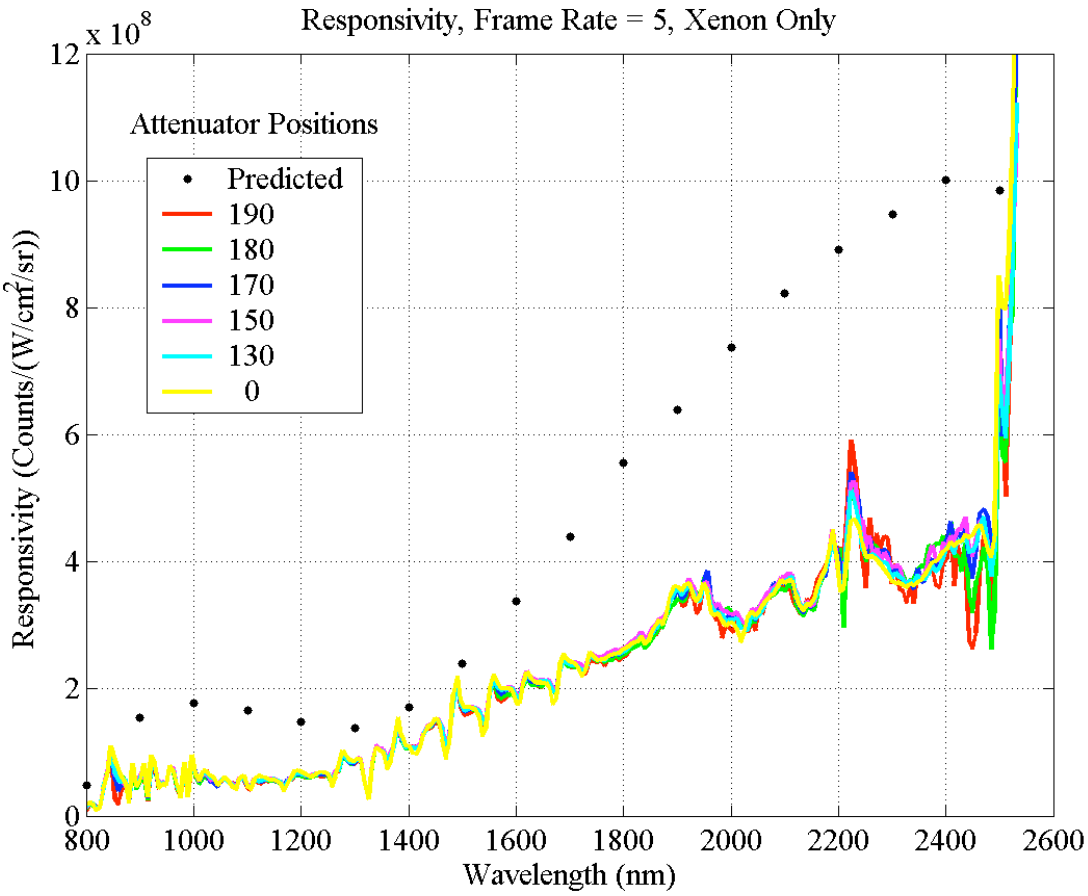

Figure 8: Responsivity of CRISP using the xenon lamp. Data from the 6 attenuator settings show consistent results. The measured responsivity is about a factor of 2 less than the predicted.

Figure 9 summarizes the responsivity results. The halogen, xenon, and joint results are plotted for multiple attenuator settings. The curves have a similar shape and are about 2 times less than the predicted results.

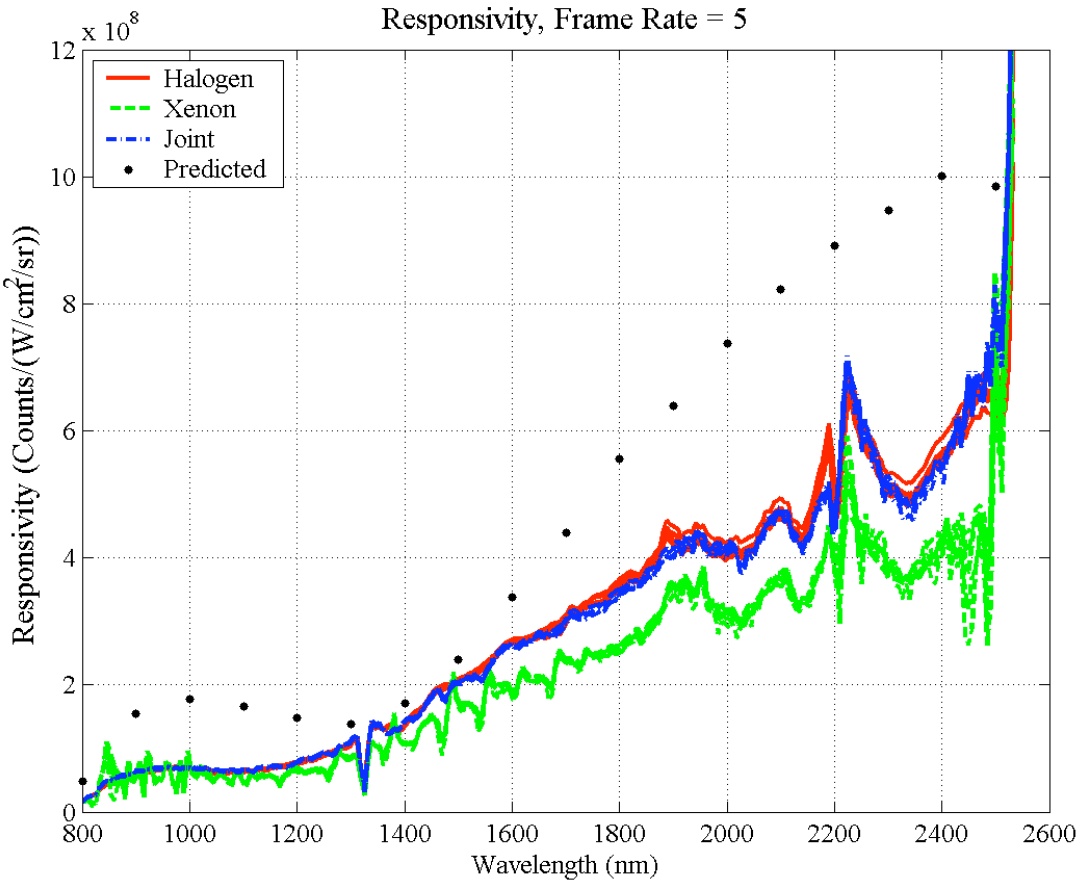

Figure 9: Summary of responsivity results for the halogen, xenon, and joint lamp configurations. The data from the xenon lamp show a lower responsivity than the halogen data.

Note that there are consistent high-frequency details to the spectrum at 1900 and 2200 nm. The sphere was calibrated in Florida in spring/summer but used here in winter. Spectralon, used to line the sphere, is known to absorb water. Addition of more water to the sphere lining (lowering the sphere radiance as calibrated, relative to what it produced at APL during CRISP calibration) could explain the 1900 nm hump. A physical mechanism for the hump at 2200 nm is not obvious, but it does coincide with a strong absorption in the fused silica window.

Conclusions

The responsivity of the CRISP instrument has been measured using the sensor images of the integrating sphere and the high-resolution calibration data for the sphere. Consistent results were seen over multiple attenuator settings. The results for the halogen, xenon, and joint lamp configurations all show a responsivity measuring about _ of the prediction.

There are some concerns about the accuracy of the sphere calibration for use in the responsivity calculations. Between the time of the CRISP tests and the sphere calibration, the halogen lamp burned out. Thus, the sphere calibration was performed with a replacement lamp that could have significant difference in the output radiance. Similarly, between the CRISP tests and the sphere calibration, the xenon lamp showed signs of wear. To overcome these differences, the sphere calibration data were scaled to match the photometer measurements from the CRISP tests. In future tests, it would be desirable to calibrate the test equipment and collect the sensor data during the same test series, to avoid these variations in the condition of the test equipment.

L. M. Howser

Distribution:

S. A. Gearhart
B. L. Gotwols
L. M. Howser
D. C. Humm
M. J. Mayr
R.W. McEntire
S. L. Murchie
E. W. Rogala
W. J. Tropf
J. W. Warren
A1F Files
Archives